Organization of Inorganic Nanomaterials *via* Programmable DNA Self-Assembly and Peptide Molecular Recognition

Joshua D. Carter[‡,⊥] and Thomas H. LaBean[†,‡,§,*]

[†]Departments of Computer Science, [‡]Chemistry, and [§]Biomedical Engineering, Duke University, Durham North Carolina 27708, United States

[⊥]Current address: Synthesis and Formulations Branch, Naval Air Warfare Center, Weapons Division, China Lake, California 93555, United States

ABSTRACT An interesting alternative to top-down nanofabrication is to imitate biology, where nanoscale materials frequently integrate organic molecules for self-assembly and molecular recognition with ordered, inorganic minerals to achieve mechanical, sensory, or other advantageous functions. Using biological systems as inspiration, researchers have sought to mimic the nanoscale composite materials produced in nature. Here, we describe a combination of self-assembly, molecular recognition, and templating, relying on an oligonucleotide covalently conjugated to a high-affinity gold-binding peptide. After integration of the peptide-coupled DNA into a self-assembling superstructure, the templated peptides recognize and bind gold nanoparticles. In addition to providing new ways of building functional multinanoparticle systems, this work provides experimental proof that a single peptide molecule is sufficient for immobilization of a nanoparticle. This molecular construction strategy, combining DNA assembly and peptide recognition, can be thought of as programmable, granular, artificial biomineralization. We also describe the important observation that the addition of 1−2% Tween 20 surfactant to the solution during gold particle binding allows the gold nanoparticles to remain soluble within the magnesium-containing DNA assembly buffer under conditions that usually lead to the aggregation and precipitation of the nanoparticles.

KEYWORDS: molecular self-assembly · structural DNA nanotechnology · molecular recognition · GEPI · oligonucleotide · oligopeptide

The future of nanoscale device fabrication for diverse applications including electronics, tissue engineering, biomedical imaging, drug delivery, catalysis, and photonics will likely require 3D constructs containing inorganic nanomaterials with tunable spacings as well as integrated organic subunits.[1−5] Such fabrication tasks are difficult for existing top-down and bottom-up fabrication strategies.[6,7] Another approach is to imitate biology, where there are numerous examples of nanoscale materials that integrate organic molecules for self-assembly and molecular recognition with ordered, inorganic minerals to achieve mechanical, sensory, or other advantageous functions. Using biological systems as inspiration, researchers have sought to mimic the nanoscale hybrid materials produced in nature. Here, we describe a new combination of self-assembly, molecular recognition, and templating, relying on a covalent conjugate[8] between an oligonucleotide and a high-affinity gold-binding peptide (selected from a combinatorial library).[9] After integration of the peptide-coupled DNA into a self-assembling superstructure, the templated peptides recognize and bind gold nanoparticles. In addition to providing new ways of building functional multinanoparticle systems, this work provides experimental proof that a single peptide molecule is sufficient for immobilization of a nanoparticle. This molecular construction strategy, combining DNA assembly and peptide recognition, can be thought of as programmable, granular, artificial biomineralization.

RESULTS AND DISCUSSION

The basis for our "molecular erector set" is the novel combination of two developing technologies, structural DNA nanotechnology,[10,11] and *in vitro* evolution of peptides for recognition of specific inorganic minerals.[7] The self-assembling DNA template used in these experiments is based on a 4 × 4 cross-tile system developed for creation of two-dimensional (2D) nanogrids displaying periodic square cavities.[12,13] Assembly of the original structure relies on two DNA tile types (types A and B) composed of nine oligonucleotides each, where each tile features one core oligonucleotide anchoring all four tile arms and the arms carry sticky-end overhangs that are designed to be complementary to exactly one sticky end on the other tile (see the Methods section for details and sequences).

* Address correspondence to thomas.labean@duke.edu.

Received for review December 9, 2010 and accepted February 2, 2011.

Published online February 11, 2011
10.1021/nn1033983

An important modification to the original design is the addition of a nick into the core DNA strand anchored in one of the tile types (tile type A). The added nick divides the original 100 nucleotide core strand into two fragments of 58 and 42 nucleotides in length, exposing a 5′ end on the shorter fragment and a 3′ end on the longer fragment. To prove the ability of individual peptides to recognize and bind gold nanoparticles, a single copy of the peptide was added to each A tile in the opening created by the nick, shown schematically in Figure 1a.[8] To ensure the entire peptide is free to participate in the gold recognition process, a spacer, in the form of two thymine nucleotides, was added between the peptide and the end of the normal core strand DNA sequence. The 5′ end of the TT spacer was labeled with an amino-terminated phosphoramidite, with the amine facilitating coupling of the oligonucleotide with the C-terminal end of the peptide. One noteworthy feature of this self-assembling DNA system is the corrugated design strategy. In this design, adjacent tiles flip with respect to each other thereby improving the formation of large pieces of nanogrid through elimination of the additive effects of tile curvature.[12,13] The corrugation feature affects the orientation of each peptide as well. The location of the nick along the core strand ultimately determines the location of the covalent bond between the peptide and the oligonucleotide. The location selected in this experiment favors peptide display on only one face of tile A. As depicted in Figure 1b, corrugation of the tiles results in an alternating up−down display pattern for the peptides.

The linear dodecapeptide employed (WALRRSIRRQSY) was identified by our collaborators through a FliTrx bacterial expression system to have a high affinity for gold surfaces.[14] The N-terminus of the peptide was acetylated to prevent the addition of multiple copies of the peptide to the oligomer chain. The peptide−oligonucleotide conjugate was prepared by coupling the C-terminal end of the peptide to the 5′ amine-terminated end of the oligonucleotide.[8] Successful coupling of the peptide to the oligonucleotide fragment was verified using polyacrylamide gel electrophoresis and MALDI mass spectrometry. Incorporation of the peptide into the DNA lattice was accomplished by combining 1 equiv of the peptide−oligonucleotide conjugate with 1 equiv each of the 18 remaining oligonucleotides and heating the mixture to 90 °C then allowing it to cool to room temperature over 12 h. As shown in the tapping mode AFM image on the left-hand side of Figure 1c, neither the addition of the nick in the core strand nor the covalent linkage of the peptide negatively affected the annealed nanogrid product (imaged in annealing buffer). Omission of the peptide−oligonucleotide conjugate from the annealing reaction resulted in samples that showed no signs of nanogrid formation.

To demonstrate successful molecular recognition by the peptides after their organization by DNA self-assembly, 5 nm gold nanoparticles (AuNP) were added to the peptide-labeled DNA nanogrid. However, prior to their addition, the AuNP required treatment with a nonionic surfactant to ensure their compatibility with the DNA nanostructure environment. Self-assembling DNA nanostructures require excess cations (typically magnesium) to screen the repulsion of the negatively charged phosphate backbones in close proximity to one another.[15] In sharp contrast, commercially available citrate-coated gold AuNP easily undergo irreversible aggregation in the presence of electrolytes and cannot tolerate the 12.5 mM magnesium used for DNA nanostructure stabilization in these experiments. Typically, researchers stabilize AuNP using thiol-based monolayers that are easily altered through ligand exchange reactions.[16,17] However, desorption of a thiolate from gold is known to require about 45 kcal/mol[18] and is thus unlikely to be displaced by the peptide ($\Delta G_{ads} \approx -8.7$ kcal/mol).[14] Instead, protection of the nanoparticles was achieved through physisorption of a nonionic surfactant, polyoxyethylene (20) sorbitan monolaurate (Tween 20), to the gold surface.[19] It is hypothesized that the interaction of the Tween 20 with the surface of the AuNP is weak compared to the attraction of the genetically engineered peptide to gold, allowing the weakly adsorbed surfactant to be displaced by the incoming peptide. The AFM photo on the right-hand side of Figure 1c shows the result of adding 1 equiv of AuNP to peptide-labeled DNA nanogrid for 60 min prior to deposition on mica for imaging. All samples combining DNA with AuNP were allowed to mix in solution for a period of time prior to deposition of 3 μL of the mixture on mica, followed by a 3 min wait before addition of 60 μL buffer for tapping mode AFM analysis. The addition of imaging buffer to the mica surface significantly dilutes the excess AuNP and is expected to quench any additional binding to the peptides. In addition to Tween 20, other agents were tested for their ability to stabilize the AuNP, including polyethylene glycol (PEG), bovine serum albumin (BSA), and polyoxyethylene (60) sorbitan monostearate (Tween 60). However, none of these were as successful as Tween 20 in stabilizing the AuNP. The optimal Tween 20 concentration was identified by testing concentrations ranging between 0.1% and 5% (w/v) for their ability to inhibit nanoparticle aggregation in 12.5 mM Mg^{2+}. At the highest nanoparticle concentration used for this report (332 nM), no aggregation was observed after several hours in magnesium containing buffer with 2% Tween 20, and all subsequent measurements were performed at this Tween 20 concentration.

Experimental evidence suggested an inverse correlation between the number of equivalents of added AuNP and the binding time required to reach

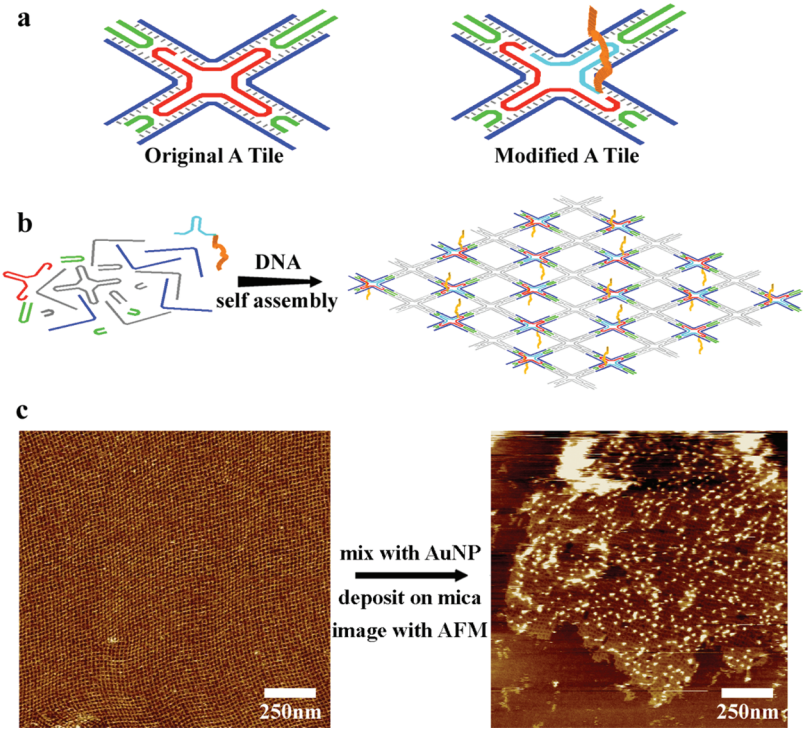

Figure 1. Peptide-modified oligonucleotides self-assemble into a grid-style lattice for organization of AuNP. (a) Schematic of the A tile original and modified designs. The modified A tile (right) shows the location of the nick and covalent addition of the gold binding peptide. (b) Self-assembly of the 19 unique oligonucleotides into a square lattice where alternating peptides display on opposing sides of the DNA lattice plane. (c) Tapping mode AFM images under buffer of DNA lattice functionalized with peptide before (left) and after (right) 1 equiv of 5 nm AuNP has been allowed to bind for 60 min. AuNP treated samples were allowed to mix in solution prior to deposition on mica and immediate AFM analysis.

near-saturating conditions. Figure 2a shows the result when 4 equiv of AuNP are added to peptide-labeled nanogrid and allowed to mix in solution for 3 min. The resulting density of templated AuNP in Figure 2a is similar to the sample pictured in Figure 1c. However, similar density was achieved for the sample with reduced AuNP concentration only after allowing mixing for much longer time. Figure 2b demonstrates this effect with even greater contrast. For this sample, 20 equiv of AuNP was added to the peptide-labeled nanogrid and allowed to mix in solution for 30 min. The resulting sample was so densely populated with AuNP that characterization was limited to low magnification images (as in Figure 2b). High magnification scans of samples with dense AuNP coverage, such as the sample shown in Figure 2b, resulted in poor image quality due to degradation of the DNA template. The dearth of unbound AuNP observed on the mica substrate is also noteworthy. The sharp contrast between the number of AuNP bound to DNA lattice *versus* the number of AuNP distributed randomly on bare mica (as shown in Figure 1c and 2b) was not observed for control lattice samples assembled without peptide.

The corrugation strategy employed in this self-assembling DNA nanostructure results in lines of peptides alternating between each face of the 2D DNA

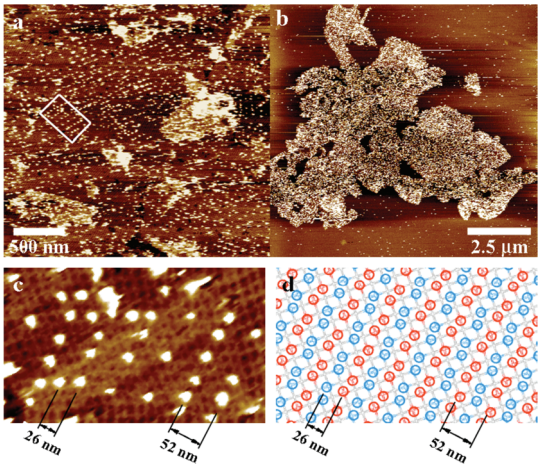

Figure 2. AuNP bound to peptide-labeled DNA lattice. (a) Rows of AuNP on peptide-labeled DNA lattice after 4 equiv of nanoparticles is allowed to bind to the peptide for 3 min before deposition into the surface. The box-outlined region depicts the magnified area shown in panel c. (b) Dense coverage of AuNP on DNA nanogrid is achieved after 20 equiv AuNP is allowed to bind for 30 min before imaging. Very few unbound AuNP particles are detectable on the exposed mica surface. (c) Magnified AFM image of the box-outlined region in panel a. Comparison of the AFM image with the map (d) shows AuNP binding favors one peptide orientation (red) over the other (blue). The map depicts peptides displayed on opposing sides of the gray-colored 2D DNA lattice as red and blue circles. The predicted distances between rows of AuNP shown in panel d correspond well with the measured distances in panel c.

lattice (depicted in Figure 1b and as red circles on one face and blue circles on the opposite face in Figure 2c). Thus, when mixed in solution, as with the samples in these experiments, AuNP should bind to both sides of the plane formed by the DNA lattice. However, comparison of the DNA lattice populated with AuNP depicted in Figure 2c with the corresponding schematic map in Figure 2d showing all possible binding sites (red and blue circles) in a similarly sized region of DNA lattice, clearly demonstrates that binding of the AuNP favors peptide rows spaced 52 nm apart. This distance represents predominately one of the two possible peptide configurations. The map shown in Figure 2d shows peptide rows displayed on the same side of the DNA lattice are 52 nm apart, while rows formed by peptides on opposing faces of the DNA lattice are 26 nm apart. The bias for AuNP binding to peptides on the same face of the DNA lattice shown in Figure 2c could be a result of the 3 min wait after deposition of the DNA lattice on the mica before dilution with imaging buffer. AuNP access to the peptides during these 3 min may be limited to the face of the DNA lattice not obscured by the mica surface. This possibility was tested by altering the sample preparation procedure. The DNA lattice was deposited on mica for 3 min before gold nanoparticles were added and allowed to bind for up to 2 h. However, this change resulted in a significantly reduced yield of AuNP binding to either configuration of peptide and did not result in a measurable bias. The observation that very little binding takes place when the DNA lattice mobility is restricted on the 2D mica surface suggests that other mechanisms might be affecting behavior of the system. In a published study of ssDNA-labeled AuNP binding to ssDNA on a DNA lattice, the authors observed a tendency for the particles to preferentially occupy nonadjacent binding sites and attributed the observation to electrostatic repulsion between negatively charged AuNP.[20] The extent to which electrostatic repulsion *versus* other mechanisms is operating in the current system remains an open question.

Detailed analysis of the experimental data shown in Figure 2c as well as additional similar results, leads to another interesting and important conclusion. The instances of AuNP binding to adjacent binding sites on peptide-labeled DNA tiles, together with clear evidence that the DNA nanogrid is lying flat (as opposed to folding or warping that would allow multiple peptides to cluster together), lead us to conclude that a single peptide molecule is sufficient to immobilize an AuNP. The AFM image in Figure 2c clearly supports this conclusion. This is the strongest experimental evidence to date supporting the contention that a single copy of the peptide binds to and immobilizes a single nanoparticle target.

We used polyacrylamide gel electrophoresis to characterize the binding of individual peptide–oligonucleotide conjugates to AuNP in measurements similar to those performed on AuNP mixed with thiolated oligonucleotides.[21] However, no change in mobility was observed between peptide–oligonucleotide conjugates with and without gold (data not shown). This result suggests that the interaction between gold and peptide, unlike Au–S, must be too weak to survive the forces exerted during electrophoresis. Furthermore, we tested the selectivity of the peptide–oligonucleotide conjugate by adding silver nanoparticles to the peptide-labeled DNA lattice. No immobilized silver nanoparticles were observed in the course of this measurement, demonstrating the high selectivity of the peptide interaction. In addition, we tested the binding of a variety of different gold particles including 1, 3, 5, 15, and 20 nm sizes, however the best initial results were obtained with 5 nm gold particles, therefore none of the other sizes were pursued in later studies.

CONCLUSION

Many imaginative future applications of nanotechnology have been envisioned. One obstacle to realizing these visions is that we are still unable to organize many of the components needed for these applications. The high-yield and high-fidelity organization of gold nanoparticles has been achieved with the simple marriage of gold and thiol chemistry with single-stranded DNA complementary to strands incorporated into DNA lattices.[20,22,23] This technique can be extended to organize additional inorganic materials using other well-known chemistries; however, the simultaneous organization of multiple inorganic species for parallel device construction favors an approach with greater selectivity, such as those exhibited by proteins in biological chemistry. This study represents the first combination of DNA-based self-assembly and peptide molecular recognition to demonstrate patterned synthetic biomineralization. With continued development, the prototype described here can be used to construct simple nanoelectronic devices, such as single electron transistors.[24] For more sophisticated assemblies, polyvalency can be included using multiple copies of the same peptide on the 5′ and 3′ oligonucleotide ends available in the nick site of the core strand. Further complexity may be achieved with the inclusion of multiple peptides capable of independently targeting different, specific materials, such as quantum dots, or semiconducting carbon nanotubes. To further develop this construction kit as an artificial, programmable biomineralization system, perhaps peptides with metal reducing capabilities may be incorporated for assembly of devices from the *in situ* nucleation and growth of nanoparticles in mild conditions from dilute ionic solutions. Some efforts in that direction have already yielded promising results, although not with the level of template complexity and programmability demonstrated here.[25,26]

METHODS

Purification of Oligonucleotides. Synthetic oligonucleotide were purchased from Integrated DNA Technologies (Coralville, IA) and separated from truncation products by denaturing polyacrylamide gel electrophoresis (PAGE). Denaturing PAGE was carried out on a 160 × 180 × 1.5 mm^3 gel containing 10% acrylamide and 8.3 M urea in TBE buffer (90 mM Tris, 90 mM boric acid, and 2 mM ethylenediaminetetraacetate (EDTA), pH 8). The gel loading buffer contained 90% formamide and 0.1% bromophenol blue. After electrophoresis (300 V for 45 min), the portion of the gel containing the desired DNA was excised, diced, and shaken overnight at 4 °C in 500 μL 0.5 M ammonium acetate, 10 mM magnesium acetate, and 2 mM EDTA. The supernatant was removed and added to a centrifuge tube with 1 mL of 200 proof ethanol and stored at −20 °C overnight. The mixture was centrifuged for 30 min at 4 °C and 16000*g* and the supernatant was discarded. The purified pellet of DNA was dissolved in pure water and the concentration was determined by ultraviolet absorption at 260 nm wavelength.

Peptide Synthesis and Purification. The peptide (Ac−WALRRSIRRQSY−OH) was synthesized on Wang resin preloaded with Fmoc-L-tyrosine (Novabiochem) at 0.1 mmol scale using a Protein Technologies PS3 automated peptide synthesizer. The coupling of standard Fmoc (9-fluorenylmethoxycarbonyl)-protected amino acids (Chem-Impex) was achieved with HBTU (*O*-benzotriazole-*N*,*N*,*N*′,*N*′-tetramethyluronium hexafluorophosphate; Novabiochem) in the presence of *N*-methylmorpholine (NMM) in *N*,*N*′-dimethylformamide (DMF) for 20 min cycles. Fmoc deprotection was achieved using 20% piperidine in DMF (2 × 5 min). The N-terminus of the peptide was acetylated with acetic anhydride and NMM. Side-chain deprotection and peptide cleavage from the resin were achieved by treating the resin-bound peptide with 5 mL of 100% trifluoroacetic acid (TFA) for 2 h under N2. After evaporation of TFA under N2, the peptide was washed three times with cold diethyl ether, air-dried, and purified by semipreparative reverse-phase HPLC on a YMC C18 column with a linear 40-min gradient from 3 to 70% acetonitrile in water with 0.1% TFA. The mass of the peptide was confirmed using an Agilent ESI-MS.

General Procedure for DMTMM Coupling Reactions in Water. DMTMM (4-(4,6-dimethoxy[1,3,5]triazin-2-yl)-4-methyl-morpholinium chloride) coupling reactions were run in 200 mM MOPS buffer pH 7.0 (200 mM (3[*N*-morpholino]propanesulfonic acid, 20 mM sodium acetate, 10 mM EDTA). A 450 pmol portion of DNA was combined with peptide (270 nmol, 600 equiv) and DMTMM (4.5 μmol, 10,000 equiv).

Workup for Coupling Reactions. The peptide−oligonucleotide conjugates were isolated from the completed solution-phase coupling reactions *via* ethanol precipitation. In this case, 1 mL of 200-proof ethanol and 50 μL of 3 M sodium acetate (150 μmoles) were added and allowed to sit overnight at −20 °C. The precipitated conjugate was centrifuged for 30 min at 4 °C and 16000*g*, and the supernatant was discarded. The pellet was dried in a vacuum centrifuge for 2 h before resuspension in 30 μL of water.

Purification of Peptide−Oligonucleotide Conjugate. Peptide−oligonucleotide conjugate (WALRRSIRRQSY - TTGTG AAGTT TTTCG ATCCT AGCAC CTCTG GAGTT TTTCT TGCC) was separated from unreacted DNA by denaturing polyacrylamide gel electrophoresis. The 30 μL fraction of resuspended reaction product was combined with 30 μL of gel-loading buffer and heated to 90 °C for 5 min before loading on to the gel. After electrophoresis (300 V for 45 min), the portion of the gel containing the peptide−oligonucleotide conjugate was excised, diced, and shaken overnight at 4 °C in 500 μLof 0.5 M ammonium acetate, 10 mM magnesium acetate, and 2 mM EDTA. The supernatant was removed and added to a centrifuge tube with 1 mL of 200 proof ethanol and stored at −20 °C overnight. The mixture was centrifuged for 30 min at 4 °C and 16000*g*, and the supernatant was discarded. The purified pellet of peptide−oligonucleotide conjugate was dissolved in pure water to a concentration of 30 μM. The final concentration was confirmed by ultraviolet absorption at 260 nm wavelength.

MALDI Analysis of Peptide−Oligonucleotide Conjugates. MALDI-TOF mass spectrometry analysis was used to characterize the oligonucleotide starting material and peptide−oligonucleotide reaction product (see Supporting Information for spectra). The analysis was performed using an Applied Biosystems DE-Pro Maldi-MS in the Mass Spectrometry Facility in the Chemistry Department at Duke University. To prepare the samples, the products were recovered from the polyacrylamide gels and dissolved in pure water to a concentration of 30 μM. Ten μL volumes of the recovered gel products were then stripped of cations using Ziptips (SCX, Millipore) and added to a mixture of 9 μL of 50 mg/mL 3-hydroxypicolinic acid and 1 μL of 50 mg/mL diammonium citrate. The mass spectrometer was run in negative-ion mode, and spectra were collected through the summing of 50 laser pulses.

DNA Strands. The DNA strands for Tile A and Tile B are shown in Tables 1 and 2.

DNA Nanostructure Formation. For DNA nanogrid formation, 18 individual standard DNA oligos and the peptide-oligo conjugate (POC) were mixed together stoichiometrically at 1.0 μM in 1× TAE/Mg2+ buffer (40 mM Tris-HCl (pH 8.0), 20 mM acetic acid, 2 mM EDTA, and 12.5 mM magnesium acetate) and slowly cooled from 95 to 20 °C over a period of 16 h. For AFM imaging, 3 μL of sample was spotted on freshly cleaved mica for 3 min. A 30μL portion of 1X TAE/Mg2+ buffer was then placed onto the mica and another 30 μL of 1X TAE/Mg2+ buffer was placed onto the AFM tip (for a total of 60 μL). AFM images were obtained on a Digital Instruments Nanoscope IIIa with a multimode head by tapping mode under buffer using NP-S tips (Veeco Inc.).

AuNP Preparation. Gold nanoparticles (AuNP, 5 nm) were purchased from Ted Pella (product no. 15702-20). To ensure AuNP stability in the high salt environment, the nanoparticles were pretreated with a nonionic surfactant. For cases in which Tween 20 or Tween 60 (Sigma Aldrich product nos. P1379 and P1629, respectively) were used, 1 mL of stock AuNP solution was mixed with the appropriate amount of stabilizing agent to achieve final Tween concentrations ranging between 0.1% and 5% (w/v). After addition of the appropriate stabilizing agent, the AuNP solutions were mixed overnight at room temperature. After incubation, the AuNP particles were concentrated, and excess stabilizing agent was removed by 6 h of centrifugation at 16000*g*. The resulting AuNP pellet was then isolated using a pipet and resuspended in 10 μL of supernatant. The concentrations of the AuNP were determined using the AuNP absorbance at 520 nm (ε520 nm for 5 nm AuNP = 1 × 107 M^{-1} cm^{-1}).[27]

AFM Imaging of AuNP-Labeled DNA Nanogrid. AuNP-labeled DNA nanogrid was prepared by adding 0.5 μL of annealed nanogrid solution to 6 μL of concentrated AuNP in 1X TAE/Mg2+ buffer. Unless noted otherwise, all samples combining DNA with AuNP were allowed to mix in solution for a specified period of time prior to deposition of 3 μL of the mixture on mica, followed by a 3 min wait before the addition of 60 μL of buffer for tapping

TABLE 1. DNA Strands for Tile A

strand name	DNA strand sequences (5′ → 3′) (bold italic text is peptide sequence)
4 × 4−1N	GGCGTGTGGTTGC
AFC2	GAGCGCAACCTGCCTGGCAAGACTCCAGAGGACTACTCATCCGT
3	GGATAGCGCCTGATCGGAACGCCTACGATGGACACGCCGACC
A44	TCACGACGGATGAGTAGTGGGCTCAGTCGGATGAGC
C5	TCCGACTGAGCCCTGCTAGGATCGACTTCACTGGACCGTTCTACCGA
C6	CTCGCTCGGTAGAACGGTGGAAGCCTCCGGTGCATG
AFC7	ACCGGAGGCTTCCTGTACGGCAGAACTCCGTTGGACGAACACTCC
4 × 4−8N	TGTTCGTGGCGCT
A9.5	AGGCACCATCGTAGGTTTTCGTTCCGATCACCAACGGAGTT-TTTTCTGCCGTACACCA
amine-labeled	/5AmMC6/TTGTGAAGTTTTTCGATCCTAGCACCTCTGGAGTTTTTCTTGCC
POC	***WALRRSIRRQSY***—TTGTGAAGTTTTTCGATCCTAGCACCTCTGGAGTTTTTCTTGCC

TABLE 2. DNA Strands for Tile B

strand name	DNA strand sequences (5′ → 3′)
B1=BB1	GCGAGGGTAGCGTGGGTAATCCATGC
BFC2	GATTACCCTGTTACCGTCGAGAAGGCCGGACCGTTCTACC
BB3	GATGTACCTGTCTCACTCGCGAGCGAAGGACGCTACC
4 × 4−6N	GCTCGGTAGAACGGTGGAAGCCAACGGTC
BFC5	GTTGGCTTCCTGACACTATCGAGATGATAGGACTACTCATCC
4 × 4−4N	ATCCGGATGAGTAGTGGGCTCAGTCGGAG
BFC7	GACTGAGCCCTGGTCTCGTCAAGGTCGGCGGACTCTATC
B88	CGTGAGATAGAGTGGTACATCGCTCA
B9	TAACACCTTCGCTCGTTTTCGAGTGAGACACCGCCGACCTTTTTTGACGAGACCACCTATCATCTTTTTCGATAGTGTCACCGGCCTTCTTTTTCGACGG

mode AFM analysis. AFM images were obtained on a Digital Instruments Nanoscope IIIa with a multimode head by tapping mode under buffer using NP-S tips (Veeco Inc.).

Acknowledgment. This work was supported by the National Science Foundation (BMAT-0706397 and EMT-0829749 to T.H.L.), by the National Institutes of Health (training Grant NIH-EB01630) and by the Office of Naval Research (N00014-09-1-0249). The authors thank Mehmet Sarikaya, Candan Tamerler, and Marketa Hnilova for assistance and valuable discussions regarding the gold-binding peptide. Correspondence and requests for materials should be addressed to T.H.L.

Supporting Information Available: MALSI_TOF analysis; height measurement of AuNP using AFM. This material is available free of charge *via* the Internet at http://pubs.acs.org.

REFERENCES AND NOTES

1. Burda, C.; Chen, X. B.; Narayanan, R.; El-Sayed, M. A. Chemistry and Properties of Nanocrystals of Different Shapes. *Chem. Rev.* **2005,** *105*, 1025–1102.
2. Leduc, P. R.; Wong, M. S.; Ferreira, P. M.; Groff, R. E.; Haslinger, K.; Koonce, M. P.; Lee, W. Y.; Love, J. C.; McCammon, J. A.; *et al.* Towards an *in Vivo* Biologically Inspired Nanofactory. *Nat. Nanotechnol.* **2007,** *2*, 3–7.
3. Lu, W.; Lieber, C. M. Nanoelectronics from the Bottom Up. *Nat. Mater.* **2007,** *6*, 841–850.
4. Zhang, Q.; Atay, T.; Tischler, J. R.; Bradley, M. S.; Bulovic, V.; Nurmikko, A. V. Highly Efficient Resonant Coupling of Optical Excitations in Hybrid Organic/Inorganic Semiconductor Nanostructures. *Nat. Nanotechnol.* **2007,** *2*, 555–559.
5. Moutos, F. T.; Guilak, F. Composite Scaffolds for Cartilage Tissue Engineering. *Biorheology* **2008,** *45*, 501–12.
6. Wang, D. Y.; Mohwald, H. Template-Directed Colloidal Self-Assembly—The Route to 'Top-Down' Nanochemical Engineering. *J. Mater. Chem.* **2004,** *14*, 459–468.
7. Tamerler, C.; Sarikaya, M., Molecular Biomimetics: Linking Polypeptides to Inorganic Structures. In *Microbial Bionanotechnology*; Rehm, B., Ed.; Horizon Bioscience: Wymondham, UK, 2006; pp 191−221.
8. Carter, J. D.; LaBean, T. H., Comparison of Coupling Reagents in the Solid-Phase and Solution-Phase Fragment-Coupling Synthesis of a Peptide-Oligonucleotide Conjugate. Submitted.
9. Sarikaya, M.; Tamerler, C.; Jen, A. K. Y.; Schulten, K.; Baneyx, F. Molecular Biomimetics: Nanotechnology Through Biology. *Nat. Mater.* **2003,** *2*, 577–585.
10. Seeman, N. C. DNA in a Material World. *Nature* **2003,** *421*, 427–431.
11. Li, H. Y.; Carter, J. D.; LaBean, T. H. Nanofabrication by DNA Self-Assembly. *Mater. Today* **2009,** *12*, 20–28.
12. Yan, H.; Park, S. H.; Finkelstein, G.; Reif, J. H.; LaBean, T. H. DNA-Templated Self-Assembly of Protein Arrays and Highly Conductive Nanowires. *Science* **2003,** *301*, 1882–1884.
13. Park, S. H.; Yin, P.; Liu, Y.; Reif, J. H.; LaBean, T. H.; Yan, H. Programmable DNA Self-Assemblies for Nanoscale Organization of Ligands and Proteins. *Nano Lett.* **2005,** *5*, 729–733.
14. Hnilova, M.; Oren, E. E.; Seker, U. O. S.; Wilson, B. R.; Collino, S.; Evans, J. S.; Tamerler, C.; Sarikaya, M. Effect of Molecular Conformations on the Adsorption Behavior of Gold-Binding Peptides. *Langmuir* **2008,** *24*, 12440–12445.
15. Sharma, J.; Chhabra, R.; Liu, Y.; Ke, Y. G.; Yan, H. DNA-Templated Self-Assembly of Two-Dimensional and Periodical Gold Nanoparticle Arrays. *Angew. Chem., Int. Ed.* **2006,** *45*, 730–735.
16. Brown, L. O.; Hutchison, J. E. Convenient Preparation of Stable, Narrow-Dispersity, Gold Nanocrystals by Ligand Exchange Reactions. *J. Am. Chem. Soc.* **1997,** *119*, 12384–12385.
17. Hostetler, M. J.; Templeton, A. C.; Murray, R. W. Dynamics of Place-Exchange Reactions on Monolayer-Protected Gold Cluster Molecules. *Langmuir* **1999,** *15*, 3782–3789.
18. Langry, K. C.; Ratto, T. V.; Rudd, R. E.; McElfresh, M. W. The AFM Measured Force Required to Rupture the Dithiolate Linkage of Thioctic Acid to Gold is Less Than the Rupture Force of a Simple Gold−Alkyl Thiolate Bond. *Langmuir* **2005,** *21*, 12064–12067.
19. Aslan, K.; Perez-Luna, V. H. Surface Modification of Colloidal Gold by Chemisorption of Alkanethiols in the Presence of a Nonionic Surfactant. *Langmuir* **2002,** *18*, 6059–6065.
20. Zhang, J.; Liu, Y.; Ke, Y.; Yan, H. Periodic Square-Like Gold Nanoparticle Arrays Templated by Self-Assembled 2D DNA Nanogrids on a Surface. *Nano Lett.* **2006,** *6*, 248–251.
21. Alivisatos, A. P.; Johnsson, K. P.; Peng, X. G.; Wilson, T. E.; Loweth, C. J.; Bruchez, M. P.; Schultz, P. G. Organization of 'Nanocrystal Molecules' using DNA. *Nature* **1996,** *382*, 609–611.
22. Le, J. D.; Pinto, Y.; Seeman, N. C.; Musier-Forsyth, K.; Taton, T. A.; Kiehl, R. A. DNA-Templated Self-Assembly of Metallic Nanocomponent Arrays on a Surface. *Nano Lett.* **2005,** *4*, 2343–2347.
23. Ding, B.; Deng, Z.; Yan, H.; Cabrini, S.; Zuckermann, R. N.; Bokor, J. Gold Nanoparticle Self-Similar Chain Structure Organized by DNA Origami. *J. Am. Chem. Soc.* **2010,** *132*, 3248–3249.
24. Coskun, U. C.; Mebrahtu, H.; Huang, P. B.; Huang, J.; Sebba, D.; Biasco, A.; Makarovski, A.; Lazarides, A.; LaBean, T. H.; Finkelstein, G. Single-Electron Transistors Made by Chemical Patterning of Silicon Dioxide Substrates and Selective Deposition of Gold Nanoparticles. *Appl. Phys. Lett.* **2008,** *93*, 12301–12303.
25. Chen, C. L.; Zhang, P. J.; Rosi, N. L. A New Peptide-Based Method for the Design and Synthesis of Nanoparticle Superstructures: Construction of Highly Ordered Gold Nanoparticle Double Helices. *J. Am. Chem. Soc.* **2008,** *130*, 13555–13557.
26. Stearns, L. A.; Chhabra, R.; Sharma, J.; Liu, Y.; Petuskey, W. T.; Yan, H. Template-Directed Nucleation and Growth of Inorganic Nanoparticles on DNA Scaffolds. *Angew. Chem., Int. Ed.* **2009,** *48*, 8494–8496.
27. Taton, T. A. Preparation of Gold Nanoparticle−DNA Conjugates. *Curr. Protoc. Nucl. Acid Chem.* **2002,** 12.2.11.